Numerical optimisation of operating conditions of waste to energy

M. Kapitler, F. Kokalj & N. Samec
Faculty of Mechanical Engineering, University of Maribor, Slovenia

Abstract

The combustion process, using municipal solid waste (MSW) as a fuel in waste to energy plant, calls for a detailed understanding of these phenomena. On the one hand, this process depends on many input parameters, like MSW proximate and ultimate analysis, the season of the year, primary and secondary inlet air velocity and, on the other hand, on the output parameters such as temperature or mass flow rate of combustion products on the exhaust. The variability and mutual dependence of these parameters can be difficult to manage in practice. Moreover, another problem is how these parameters can be tuned to achieve the optimal combustion with minimal pollutants emission during the plant design phase already. To meet these goals, a waste to energy plant with bed combustion is investigated by using a computational fluid dynamics approach with ANSYS CFX 12.0 code in WORKBENCH 2 environment. In this paper, the adequate variable input boundary conditions which are based on the real measurement and practical calculations of known MSW composition from other authors are used and the whole computational work is updated with real plant geometry and the appropriate turbulence, combustion and heat transfer models. Furthermore, the operating parameters were optimized on output parameters through trade-off study. Different operating conditions were varied and the fluid flow direction, residence time, temperature field, velocity field, nitric oxide formation and combustion products through plant combustion chamber and preheat intersection in 3D were predicted and visualized. The optimization in real time has shown the amount of each input parameters to meet the optimal operating conditions. Finally, the response charts between the input and output parameters are presented to monitor the dependence among these parameters. Further simulations have to be done to include the geometry dimensions as input parameters.
Keywords: municipal solid waste modelling, bed combustion, computational fluid dynamics, operating conditions, numerical optimisation, trade-off study, parameter sensitivity, response charts.

1 Introduction

Nowadays, bed combustion on grate is the most common way to burn municipal solid waste (MSW) in waste to energy plants (WTEP). The combustion in these plants are very specific due to the characteristics of fuel (MSW) which depends on proximate and ultimate analysis, season of the year, primary and secondary inlet air velocity and many other parameters which change all the time in some frames. The goals are how the optimal combustion can be tuned with minimal emission of the pollutants in the environment already in the plant project phase. To meet these goals, WTEP with bed combustion is investigated by using computational fluid dynamics (CFD) approach [1–11] with ANSYS CFX 12.0 code in the WORKBENCH 2 environment. By using this tool the input and output parameters can be followed and the mutual interaction visualized. The mathematical models were developed like FLIC [5, 7–10] and test project TAMARA [3] to find out the combustion products distribution in the gaseous phase along the travel bed. The combustion of MSW in the gaseous phase combustion has many phases like moisture evaporation, waste devolatilisation, combustion of volatiles, mixing and fixed carbon combustion during heterogeneous chemical reactions [10].

2 Numerical optimization of operating conditions

2.1 Models description

The combustion in a WTEP is described quite accurately by a system of differential equations of the reacting flow so called Reynolds Averaged Navier-Stokes equations (RANS), presented in the following form:

$$\frac{\partial \overline{\rho}}{\partial t} + \frac{\partial}{\partial x_j}\left(\overline{\rho}\,\overline{\upsilon}_j\right) = 0 , \tag{1}$$

$$\frac{\partial}{\partial t}\left(\overline{\rho}\,\overline{\upsilon}_j\right) + \frac{\partial}{\partial x_j}\left(\overline{\rho}\,\overline{\upsilon}_j\overline{\upsilon}_i\right) = -\frac{\partial p}{\partial x_i} + \overline{f_{\upsilon i}} - \frac{\partial}{\partial x_j}\left(\overline{\tau}_{ij} + \overline{\rho\upsilon'_j\upsilon'_i}\right) , \tag{2}$$

$$\frac{\partial}{\partial t}\left(\overline{\rho}\,\overline{h}\right) + \frac{\partial}{\partial x_j}\left(\overline{\rho}\,\overline{\upsilon}_j\overline{h}\right) - \frac{\partial p}{\partial t} + \frac{\partial}{\partial x_j}\left(\overline{q}_j + \overline{\rho\upsilon'_j h'}\right) = \overline{I}_T . \tag{3}$$

Reynolds' stresses ($\overline{\rho\upsilon'_j\upsilon'_i}$) are modelled by the introduction of turbulent viscosity η_t:

$$\overline{\rho\upsilon'_j\upsilon'}_i = \frac{2}{3}\delta_{ij}\left(\rho k + \eta_t \frac{\partial \upsilon_k}{\partial x_k}\right) - \eta_t\left(\frac{\partial \upsilon_i}{\partial x_j} + \frac{\partial \upsilon_j}{\partial x_i}\right) . \tag{4}$$

The turbulent viscosity can be determined using various turbulent models to close-down the system of Reynolds' equations. The two-equation k - ε turbulent model is used for the purpose of the presented reacting flow modelling. The application of k - ε turbulent model in the modelling of reacting flows has already been proven by many authors as a very successful one. The turbulent viscosity is computed using:

$$\eta_t = \rho C_\eta \frac{k^2}{\varepsilon}, \tag{5}$$

where k is turbulent kinetic energy – $k = 0.5\left(\overline{\upsilon_i'\upsilon_i'}\right)$ and ε its dissipation (irreversible transformation of kinetic energy into internal energy).

Local values of k and ε are computed using the following transport equations:

$$\frac{\partial}{\partial t}(\rho k) + \frac{\partial}{\partial x_j}\left(\overline{\upsilon}_j k\right) - \frac{\partial}{\partial x_j}\left[\left(\eta + \frac{\eta_t}{\sigma_k}\right)\frac{\partial k}{\partial x_j}\right] = I_k, \tag{6}$$

$$\frac{\partial}{\partial t}(\rho \varepsilon) + \frac{\partial}{\partial x_j}\left(\overline{\upsilon}_j \varepsilon\right) - \frac{\partial}{\partial x_j}\left[\left(\eta + \frac{\eta_t}{\sigma_\varepsilon}\right)\frac{\partial \varepsilon}{\partial x_j}\right] = I_\varepsilon, \tag{7}$$

the source terms are modelled as:

$$I_k = \eta_t\left(\frac{\partial \overline{\upsilon}_i}{\partial x_j} + \frac{\partial \overline{\upsilon}_j}{\partial x_i}\right)\frac{\partial \overline{\upsilon}_i}{\partial x_j} - \rho\varepsilon, \tag{8}$$

$$I_\varepsilon = C_1 \frac{\varepsilon}{k}\left[\eta_t\left(\frac{\partial \overline{\upsilon}_i}{\partial x_j} + \frac{\partial \overline{\upsilon}_j}{\partial x_i}\right)\frac{\partial \overline{\upsilon}_i}{\partial x_j}\right] - C_2 \rho \frac{\varepsilon^2}{k}. \tag{9}$$

Reynolds' enthalpy flux $\overline{\rho\upsilon_j' h'}$ in eqn (3) is also defined with turbulent viscosity:

$$\overline{\rho\upsilon'_j h'} = -\frac{\eta_t}{\mathrm{Pr}_t}c_p\frac{\partial T}{\partial x_j}, \tag{10}$$

where Pr_t is the turbulent Prandtl number. C_η, C_1, C_2, σ_k and σ_ε are constants, and their values used in the presented work are: $C_\eta = 0.09$; $C_1 = 1.44$; $C_2 = 1.92$; $\sigma_k = 1$ and $\sigma_\varepsilon = 1.3$.

Advection – diffusive equation of mass species (ξ_k) of the component k has due to Reynolds' averaging, an additional term called turbulent mass species flux:

$$\overline{\rho\xi_k'\upsilon_j'} = \frac{\eta_t}{\mathrm{Sc}_t}\frac{\partial \xi_k}{\partial x_j}, \tag{11}$$

and can be modelled with turbulent viscosity using the k-ε model. The complete advection – diffusive mass species equation is:

$$\frac{\partial}{\partial t}\left(\overline{\rho\xi_k}\right)+\frac{\partial}{\partial x_j}\left(\overline{\rho\upsilon_j\xi_k}\right)-\frac{\partial}{\partial x_j}\left[\left(\rho D_k+\frac{\eta_t}{\mathrm{Sc}_t}\right)\frac{\partial\xi_k}{\partial x_j}\right]=\overline{I_{\xi_k}}\,, \qquad (12)$$

where Sc_t is the turbulent Schmidt number and D_k molecular diffusion coefficient of component k. With the new term:

$$\Gamma_{k,\mathit{eff}}=\rho D_k+\frac{\eta_t}{\mathrm{Sc}_t}=\Gamma_k+\frac{\eta_t}{\mathrm{Sc}_t}\,, \qquad (13)$$

eqn (12) can be rewritten as:

$$\frac{\partial}{\partial t}\left(\overline{\rho\xi_k}\right)+\frac{\partial}{\partial x_j}\left(\overline{\rho\upsilon_j\xi_k}\right)-\frac{\partial}{\partial x_j}\left(\Gamma_{k,\mathit{eff}}\frac{\partial\xi_k}{\partial x_j}\right)=\overline{I_{\xi_k}} \qquad (14)$$

Source terms of energy and mass species transport equations are computed by the following two equations where ω_k is computed from the turbulent combustion model:
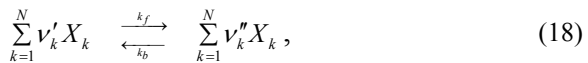
$$\overline{I_T}=-\sum_{k=1}^{N}\Delta H_{f,k}^o\,\overline{\omega}_k\,, \qquad (15)$$

$$\overline{I_{\xi_k}}=M_k\overline{\omega}_k\,, \qquad (16)$$

where $\Delta H^{\circ}_{f,k}$ is the standard heat formation and M_k the molecular mass of component k. In eqns (15) and (16), ω_k stands for the formation/consumption rate of component k and is defined by the following expression:

$$\overline{\omega}_k=\frac{d\left[X_k\right]}{dt}=\left(v_k''-v_k'\right)\overline{R}_k\,, \qquad (17)$$

which is written for the general form of the chemical reaction:

$$\sum_{k=1}^{N}v_k'X_k\;\overset{k_f}{\underset{k_b}{\rightleftarrows}}\;\sum_{k=1}^{N}v_k''X_k\,, \qquad (18)$$

where v_k' and v_k'' represent the stoichiometric coefficients of component k for reactants and products, respectively. Chemical reaction rate R_k in eqn (17) is

calculated from appropriate combustion models. It has to be pointed out that nowadays many turbulent combustion models are in practical use. Their application depends on the type of combustion (diffusion, kinetic, mixed), fuel type (solid, liquid, gaseous) and combustion device (furnace, boiler, engine). Most of models include various empirical constants which need to be individually determined case by case. In this case the Eddy Dissipation Combustion Model has been applied [12, 13].

2.2 Geometry, meshing and boundary conditions

With the CFD approach the combustion processes can be predicted and the operating condition and combustion chamber optimized in existing waste to energy power plant (WTEP) or in the project phase. Fig. 1 shows the 2D engineering plan view of WTEP.
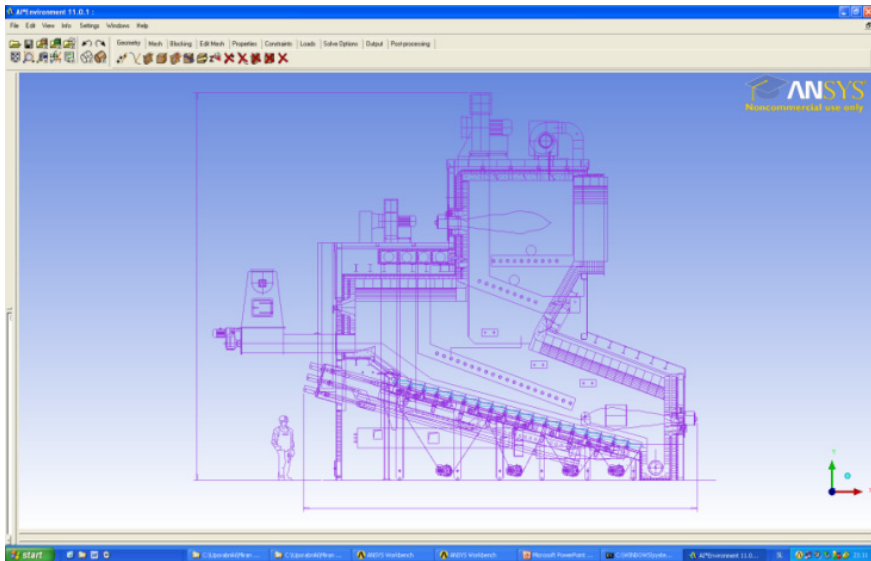

Figure 1: The 2D engineering plan view of WTEP.

On this base the WTEP was built and operates with RDF as a fuel produced with MBT from MSW. Fig. 2 shows grate, details in the primary combustion chamber with waste input (left) and the secondary combustion chamber with secondary and tertiary air inlet (right).

The 3D geometry plan on the base of engineering plans in real measure was drawn (fig. 3 – left). Each dimension was marked on the plan with corresponding input dimensions. In this way each dimension is easy and quickly modified and the entire construction can be quickly changed and redrawn.

Figure 2:   Grate in primary combustion chamber and secondary and tertiary air inlets.

Furthermore, the meshing of ca. 1.4 million cells (fig. 3, right) is created and the boundary conditions with entire combustion, radiation, particle tracking and other models, input and output parameters are set up. These input parameters are operating conditions like input velocities, temperatures, reactants mass flow rates (MFR), dimension value and the output parameters like temperatures, combustion products MFR and other exhaust parameters. It is known that the concentration of gaseous components which are created from MSW combustion like carbon monoxide, methane, hydrogen, nitrogen monoxide or oxygen above the bed are differently distributed along the grate set [3, 4, 6, 7, 9]. These facts are taken into consideration when the boundary conditions are defined. In this study, the measured operating parameters form existing WTEP is used as the input parameters (IP). In addition, the reactions for gaseous combustion are also defined and the entire model is solved. Many other authors have used the FLUENT solver code [3–11] but in this study it is interesting that the CFX V12.0 solver code in the Workbench 2 environment which was developed by Ansys, Inc. has been used [12, 13] and the results are quite similar.
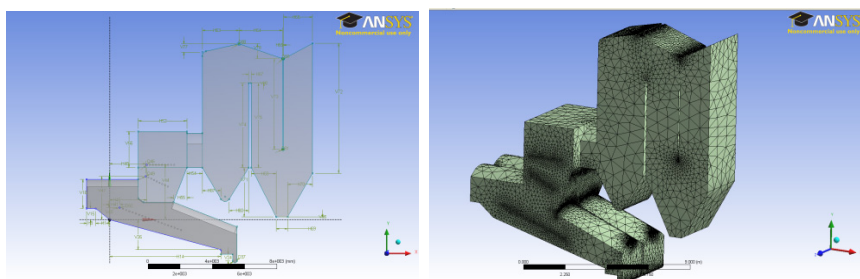

Figure 3:   3D geometry plan of WTEP with dimensions (left) and meshing (right).

The optimisation process was developed using design exploration which is a powerful tool for designing and understanding the analysis response of parts and assemblies. It is a deterministic method based on Design of Experiments (DOE) and various optimisation methods with parameters as its fundamental components. DOE techniques have one common characteristic: they try to locate the sampling points such that the space of random input parameters is explored in the most efficient way, or obtain the required information with a minimum of sampling points. Sample points in efficient locations will not only reduce the required number of sampling points, but also increase the accuracy of the response surface that is derived from the results of the sampling points. By default the deterministic method uses a central composite design, which combines one centre point, points along the axis of the input parameters and the points determined by a fractional factorial design. GDO is a constrained, multi-objective optimisation technique in which the best possible designs are obtained from a sample set given the objectives set from parameters. GDO can be used for design optimisation in three ways: the screening, the Multi-Objective Generic Algorithm (MOGA) approach and the Non-Linear Programming by Quadratic Lagrangian approach (NLPQL). The screening approach is a non-iterative direct sampling method by a quasi-random number generator based on Hammersley algorithm. MOGA approach is an iterative Multi-Objective Genetic Algorithm, which can optimize problems with continuous input parameters. NLPQL is a gradient based single objective optimizer which is based on the mathematical optimisation algorithm developed by Klaus Schittkowski. GDO has more possible objectives and they are: no-objective, minimize, maximize, and target value which is less than or equal to or greater than or equal to the input target value. The importance of the parameter is default, lower and higher. By setting these targets the three best candidates (A, B or C) are chosen which best met all the requests.

Probabilistic sensitivities are based on a statistical correlation analysis between the individual probabilistic design variables. You can review the parameters correlation data that has been used to derive sensitivities and decide if individual sensitivity values are significant or not. This information is collected in the correlation matrix of the random output parameters versus the random input variables. It can be also reviewed in the correlations that have been sampled between random input variables. The correlations between random output parameters are important if the probabilistic results of a probabilistic analysis are wanted as input for another probabilistic analysis.

When the optimisation process is finished, all results can be studied and the response charts can be visualized.

3   Results and discussion

In the study three input parameters (IP) are used: secondary air inlet velocity (InSecAirVelocity-m/s), oxygen MFR (MassInVelocity in m/s) and MWS velocity (MSWVelocity in m/s) and many other output parameters (OP): average value of following parameters at the exit of the WTEP – CO (COOut dimensionless), temperature (TempOut in Kelvin (K), CH_4 (CH4Out

dimensionless), oxygen (O2Out dimensionless); average value ash travelling time along the grate (AshTime in s), average ash temperature (AshTemp in K), maximal ash temperature through the WTEP (AshMaxTemp in K), etc.

On the other hand, it has to be ensured that the maximum ash temperature does not exceed the ash melting point and flying ash deposit on heat exchangers walls, which can cause a great damage, has to be avoided. The optimisation response chart (fig. 4), which was created as a result of DOE helps the determination of the interaction among maximal ash temperature versus secondary air velocity and oxygen MFR in the secondary air inlet. The maximal ash temperature from secondary air velocity of 27 m/s to 29 m/s increases rapidly and peaked at a maximum ash temperature of 1850 K. On the other hand, there is no significant dependence of oxygen MFR in the region from 0.255 to 0.21. In this way, the damage this phenomenon can cause can be predicted and avoided.

Table 1 shows the setting and results of trade-off optimisation with IP and OP. As can be seen, three candidates, which best match the requirements, appear with belonging values. In this way the optimisation is easy and effectively used.

Fig. 5 shows the temperature field comparison by different operating condition of oxygen MFR. The temperature in secondary combustion chamber increases when enriched air is used [6, 11].

Fig. 6 shows the sensitivities among input and output parameters. It is important to know which input parameter has an influence on which output parameter and in which role (negative or positive). As can be seen, every output parameter has a huge sensitivity to the input parameter second air velocity and the output parameters have a limited sensitivity or no sensitivity to the other input parameters.
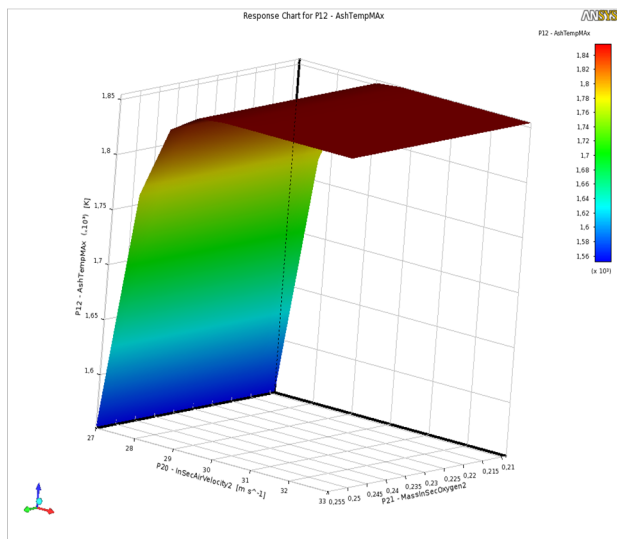

Figure 4:   Response chart for maximal ash temperature vs. secondary air velocity and oxygen MFR in secondary air inlet.

Table 1:   Trade-off study parameters objective settings and results.

Table of Schematic B4: Optimization						
▼	A	B	C	D	E	F	G
1		P20 - InSecAirVelocity2 (m s^-1)	P21 - MassInSecOxygen2	P22 - MSWVelocity (m s^-1)	P5 - COOut	P6 - TempOut (K)	P7 - COSecIn
2	Optimization Study						
3	Objective	No Objective	Minimize	No Objective	Minimize	No Objective	No Objective
4	Target Value						
5	Importance	Default	Higher	Default	Higher	Default	Default
6	GDO Sample Set 1						
7	Candidate A	30,87	0,20939	0,98001	-8,0526E-06	1104,8	0,090197
8	Candidate B	32,79	0,21012	0,95367	-7,9964E-06	1104,7	0,090201
9	Candidate C	31,83	0,21084	1,0985	-8,0161E-06	1104,8	0,0902

| H	I	J	K	L	M	N
P8 - COSecOut	P9 - CH4Out	P10 - AshTime (s)	P11 - AshTemp (K)	P12 - AshTempMAx (K)	P13 - O2Out	P14 - COVsCo2MidRAtio
No Objective	No Objective	No Objective	Minimize	No Objective	Maximize	No Objective
Default	Default	Default	Higher	Default	Higher	Default
2,0433E-05	-2,855E-06	4,9722	1174	1854,5	0,095124	0,36661
2,8447E-05	-2,835E-06	4,9729	1174	1854,3	0,095088	0,36663
2,5632E-05	-2,842E-06	4,9726	1174	1854,4	0,095101	0,36662
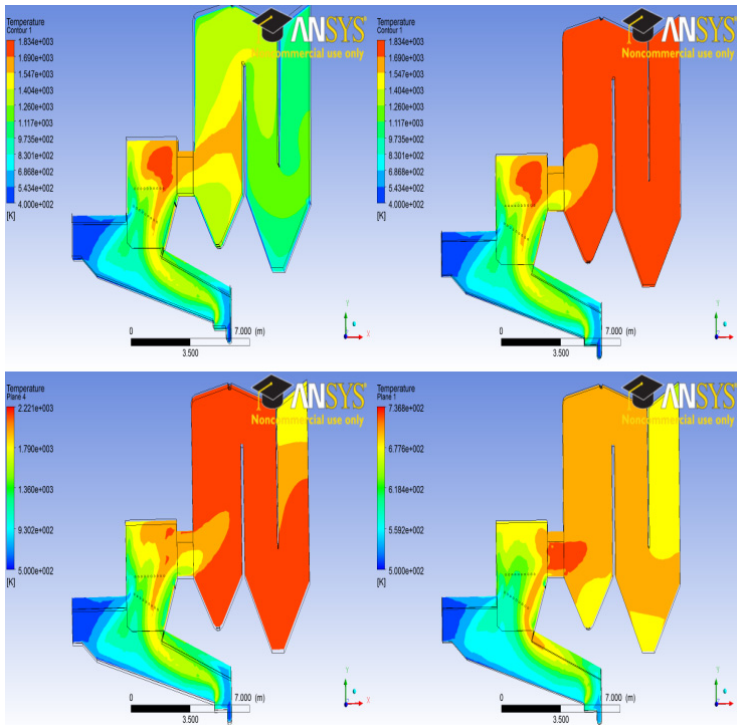
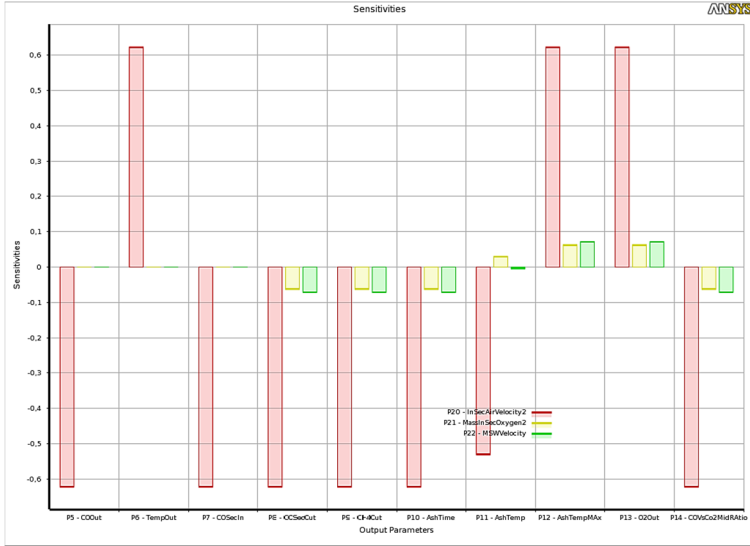Figure 5:   Temperature field by different oxygen MFR at secondary enriched air inlet.

Figure 6: Local parameters sensitivities.

Fig. 7 shows the trade-off study chart for input parameter second air velocity (InSecAirVelocity2) and the output parameter CO at the exit (COOut). The feasible points to match the criteria (table 1) are shown and the dependence of input velocity is very important. For example when a velocity of 27 m/s is used, the CO MFR at the output is 0.018 and when the velocity of 27.5 m/s is used the CO MFR is only 0.0045.
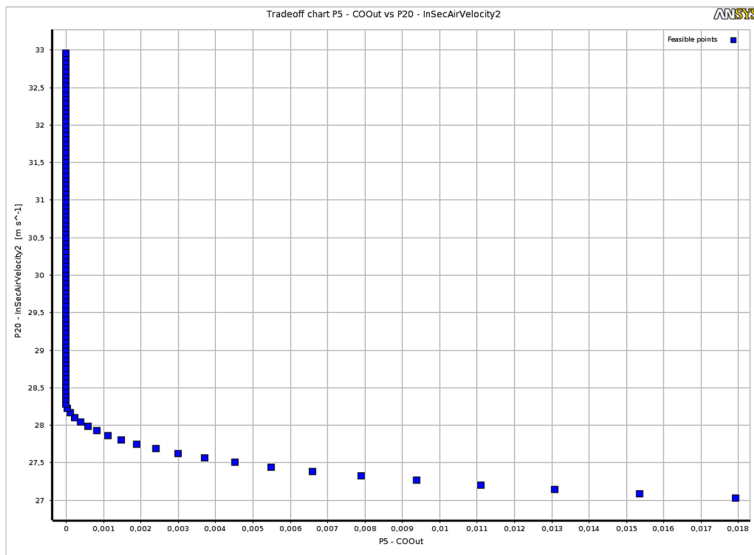

Figure 7: Trade-off chart COOut (OP) vs. second air velocity (IP).

As it can be seen, the CFD is the most convenient tool to predict the optimal conditions which have to be achieved in relation to thermal and environmental efficiency and as well as safety of the WTEP operation. With this tool, problems can also be avoided because the whole situation can be predicted with appropriate inlet boundary conditions.

4   Conclusion

The applicability of various combustion operating conditions was examined and analyzed, based on the real operating conditions. The CFD approach and the numerical optimisation was used to identify the appropriate conditions to achieve complete combustion and minimize the pollutants emission. The input and output parameters were studied and visualized in the response charts and the local sensitivities among different parameters were presented. Furthermore, the parameters correlation was identified through the parameters matrix. In the end, further simulations have to be carried out to include the geometry dimensions as input parameters.

References

[1]   Yin, C., Rosendahl, L., Kaer, S.H., Clausen, S., Hvid, S.L. & Hille, T., Mathematical modeling and experimental study of biomass combustion in a thermal 108 MW grate-fired boiler. *Energy & Fuels*, **22**, pp. 1380-1390, 2008.

[2]   Kokalj, F. & Samec, N., An analysis of the combustion conditions in the secondary chamber of a pilot-scale incinerator based on the computational fluid dynamics. *Journal of Mechanical Engineering*, **51**, pp. 280-303, 2005.

[3]   Frey, H.-H., Peters, B., Kunsinger, H. & Vehlow, J., Characterization of municipal solid waste combustion in a grate furnace. *Waste Management*, **23**, pp. 689-701, 2003.

[4]   Costa, M., Dell'Isola, M. & Massarotti, N., Numerical analysis of the thermo-fluid-dynamic field in the combustion chamber of an incinerator plant. *Energy*, **34**, pp. 2075-2086, 2009.

[5]   Anderson, S.R., Kadirkamanathan, V., Chipperfield, A., Sharifi, V. & Swithenbank, J., Multi-objective optimization of operating variables in a waste incineration plant. *Computer & Chemical Engineering*, **29**, pp. 1121-1130, 2005.

[6]   Yang, W., Nam, H.-S. & Choi, S., Improvement of operating conditions in waste incineration using engineering tools. *Waste Management*, **27**, pp. 604-613, 2007.

[7]   Yang, Y.B. & Swithenbank, J., Mathematical modelling of particle mixing effect on the combustion of municipal solid wastes in a packet-bed furnace. *Waste Management*, **28**, pp. 1290-1300, 2008.

[8]   Yang, Y.B., Sharifi, V.N. & Swithenbank, J., Converting moving-grate incineration from combustion to gasification - Numerical simulation of the burning characteristics, *Waste Management*, **27**, pp. 645-655, 2007.

[9]   Yang, Y.B., Yamauchi, H., Nasserzadeh, V. & Swithenbank, J., Effects of fuel devolatilisation on the combustion of wood chips and incineration of simulated municipal solid wastes in a packed bed. *Fuel*, **82**, pp. 2205-2221, 2003.

[10] Yang, Y.B., Goh, Y.B., Zakaria, R., Nasserzadeh, V. & Swithenbank, J., Mathematical modelling of MSW incineration on a travelling bed. *Waste management*, **22**, pp. 369-380, 2002.

[11] Yu, Z., Ma, X. & Liao, Y., Mathematical modelling of combustion in a grate-fired boiler burning straw and effect of operating conditions under air- and oxygen-enriched atmospheres. *Renewable Energy*, **35**, pp. 895-903, 2010.

[12] ANSYS, Inc., Southpointe, 275 Technology drive, Canonsburg, PA 15317, United States, Software packet Workbench 2 with CFX 12.0: Help Mode.

[13] ANSYS, Inc., Southpointe, 275 Technology drive, Canonsburg, PA 15317, United States, www.ansys.com/customerportal/index.htm